RyR1/RyR3 Chimeras Reveal that Multiple Domains of RyR1 Are Involved in Skeletal-Type E-C Coupling

Claudio F. Perez,* Andrew Voss,† Isaac N. Pessah,† and Paul D. Allen*
*Department of Anesthesiology, Perioperative and Pain Medicine, Brigham and Women's Hospital, Boston, Massachusetts; and †Department of Molecular Biosciences, University of California, Davis, California

ABSTRACT Skeletal-type E-C coupling is thought to require a direct interaction between RyR1 and the α_{1S}-DHPR. Most available evidence suggests that the cytoplasmic II–III loop of the dihydropyridine receptor (DHPR) is the primary source of the orthograde signal. However, identification of the region(s) of RyR1 involved in bidirectional signaling with the α_{1S}-DHPR remains elusive. To identify these regions we have designed a series of chimeric RyR cDNAs in which different segments of RyR1 were inserted into the corresponding region of RyR3 and expressed in dyspedic 1B5 myotubes. RyR3 provides a preferable background than RyR2 for defining domains essential for E-C coupling because it possesses less sequence homology to RyR1 than the RyR2 backbone used in previous studies. Our data show that two regions of RyR1 (chimera Ch-10 aa 1681–2641 and Ch-9 aa 2642–3770), were independently able to restore skeletal-type E-C coupling to RyR3. These two regions were further mapped and the critical RyR1 residues were 1924–2446 (Ch-21) and 2644–3223 (Ch-19). These results both support and refine the previous hypothesis that multiple domains of RyR1 combine to functionally interact with the DHPR during E-C coupling.

INTRODUCTION

Unlike type-2 and type-3 ryanodine receptors (RyR2 and RyR3, respectively) the type-1 isoform (RyR1) displays the unique property of allowing excitation-contraction (E-C) coupling in the absence of extracellular Ca^{2+}. This property is referred to as skeletal-type E-C coupling. A mechanical coupling model, in which there is a direct physical interaction between RyR1 and the α_{1S} subunit of L-type Ca^{2+} channels (dihydropyridine receptor; α_{1S}-DHPR) in the plasma membrane, has been proposed to explain this phenomenon (Rios et al., 1993; Rios and Pizarro 1991; Schneider 1994). According to this model a depolarization-induced conformational change in the DHPR, which acts as the surface membrane voltage sensor, directly transmits a signal to RyR1 causing its activation. The resulting calcium release from the sarcoplasmic reticulum (SR) is essential for contraction (Berchtold et al., 2000).

Studies in dyspedic skeletal muscle myotubes that lack expression of RyR1 have shown that there is also a ''retrograde'' signal from RyR1 to DHPR, which is responsible for enhancement of the Ca^{2+} channel activity of DHPR (Nakai et al., 1996) in addition to the orthograde signal from the DHPR to RyR1. This reciprocal bidirectional interaction appears to be RyR1-specific, since native and expressed RyR3 and expressed RyR2 lack the ability to enhance DHPR activity (Nakai et al., 1997).

Extensive studies have been focused on the identification of the molecular domains of DHPR and RyR1 involved in such bidirectional signaling. There is compelling evidence suggesting that the putative cytoplasmic loop between the intramembrane segments II and III (II–III loop) of the α_{1S} subunit of DHPR is both necessary and sufficient for normal E-C coupling. Its critical role was first recognized by Tanabe et al. (1990), who demonstrated the return of normal skeletal-type E-C coupling in dysgenic myotubes expressing chimeric cardiac DHPRs in which the cardiac II–III loop was replaced with the skeletal-type sequence. Subsequent studies have identified a 46-residue region of the skeletal II–III loop that is sufficient to both transfer strong skeletal-type E-C coupling properties to an otherwise cardiac DHPR and remove skeletal-type E-C coupling from an otherwise skeletal DHPR (Grabner et al., 1999; Nakai et al., 1998b; Wilkens et al., 2001). However, recent evidence indicates that other regions of DHPR, in addition to α_{1S} II–III loop, are able to interact with RyRs and may contribute functional interactions in signaling between DHPR and RyR1 (Leong and MacLennan 1998c; Slavik et al., 1997; Stange et al., 2001).

Whereas the studies of the region of the DHPR needed to interact with RyR1 are numerous, studies aimed at identifying the region(s) of RyR1 involved in cross talk with DHPR during E-C coupling have only recently begun. Studies of the crooked neck dwarf mutant chicken which expresses only RyR3 (Airey et al., 1993a; Ivanenko et al., 1995) and from dyspedic myotubes expressing RyR2 or RyR3 (Fessenden et al., 2000; Nakai et al., 1997), have shown that neither isoform could support skeletal-type E-C coupling. Yamazawa et al. (1997) used cultured primary myotubes from mice lacking expression of RyR1 and RyR3 to demonstrate that a mutated RyR1 in which the divergence region D2 (amino acids 1342–1406 of RyR1) was deleted could not restore skeletal-type E-C coupling. This suggested that the D2 domain contributes structural determinants important for E-C coupling in skeletal muscle.

Leong and MacLennan (1998a), using small RyR1 GST

Submitted July 3, 2002, and accepted for publication December 2, 2002.
Address reprint requests to Claudio F. Perez, Brigham and Women's Hospital, 75 Francis St., Boston, MA 02115. Tel.: 617-732-6881; Fax: 617-732-6927; E-mail: cperez@zeus.bwh.harvard.edu.

0006-3495/03/04/2655/09 $2.00

fusion proteins, identified a region of 37 amino acids, encompassing residues 1076–1112 of RyR1, that was able to interact specifically with affinity columns containing the DHPR α_{1S} II–III loop. Similarly, using affinity chromatography they reported that a GST fusion protein fragment containing residues 922–1112 of RyR1 was also able to bind to a column containing the DHPR α_{1S} III–IV loop (Leong and MacLennan, 1998c). In a more physiological approach, Nakai et al. (1998a) used chimeric RyRs to express different regions of RyR1 into an otherwise RyR2 receptor. He reported that residues 1635–2636 of RyR1 were able to both mediate skeletal-type E-C coupling and enhance DHPR channel activity. They also found that a second chimera containing the adjacent residues 2659–3720 was able to enhance DHPR channel activity but displayed no skeletal-type E-C coupling. These data suggest that at least two independent regions of RyR1 might be involved in the cross talk with DHPR. The fact that RyR1/RyR2 chimeras, which are expressed in a RyR2 background that normally is not present in skeletal muscle, were able to restored skeletal-type E-C coupling suggests that the regions identified in this study contain all the domain(s) of RyR1 required to support the skeletal-specific protein-protein interactions during E-C coupling. However, there is a body of evidence suggesting that like in skeletal muscle, a direct or indirect interaction may exist in cardiac muscle between RyR2 and α_{1C}-DHPR (Katoh et al., 2000; Mouton et al., 2001; Slavik et al., 1997). Thus, it is possible that RyR2 may display a closer similarity to RyR1 than was anticipated and therefore, the two proteins may share several common functional domains. Some of these domains may be critical for skeletal-type E-C coupling and their ''absence'' would remain undetected in the RyR1/RyR2 chimeras. In this regard, RyR3 seems to present less homology to RyR1 than RyR2 (Ottini et al., 1996; Oyamada et al., 1994), and no interaction between any DHPR and RyR3 has been described so far. Additionally, unlike RyR2, RyR3 is normally expressed in skeletal muscle. Together, this suggests that RyR3 may be a better background than RyR2 to identify specific regions of RyR1 critical for skeletal E-C coupling in chimeric receptors.

To verify whether the critical domain of RyR1 previously identified for Nakai et al. (1998a) is able to confer skeletal-type E-C coupling regardless of the background in which it is expressed, in this work we have generated a series of chimeric RyR1/RyR3 receptors and expressed them in dyspedic 1B5 myotubes which lack expression of all three RyR isoforms. We report that exchanging residues 1681–3770 of RyR1 for the corresponding residues from RyR3 allowed RyR3 to gain skeletal-type E-C coupling. Furthermore, we were able to dissect from this domain to two separate smaller regions that were independently capable of allowing RyR3 to gain skeletal-type E-C coupling. Interestingly, expression of this critical domain in an RyR3 background was less efficient in restoring E-C coupling than was previously reported in similar chimera in an RyR2 background (Nakai et al., 1998a). These data both confirm and refine previous data reported with RyR1/RyR2 chimeras, that these regions contain essential domains needed for E-C coupling and suggest that multiple regions of RyR1 are involved in its interaction with the DHPR during E-C coupling.

MATERIAL AND METHODS

Chimeric constructs

Amino acid alignments of RyR1 and RyR3 cDNAs sequences were performed to select fragments of RyR1 to be inserted into the corresponding sequence of RyR3. Specific primers were designed to amplify the selected fragments by PCR using RyR1 as a template. Each set of primers inserted a unique restriction site. Amplified fragments from RyR1 were inserted, in frame, into the endogenous restriction site(s) of HSV-RyR3 plasmid as follows (* indicates a created site, *Sk*: skeletal): Ch-10: *Bsi*WI-*Hin*dIII (Sk 5045–7930); Ch-9 *Hin*dIII-*Asc*I* (Sk 7930–11,311); Ch-17: *Bsi*WI-*Kpn*I (Sk 5045–6652); Ch-18: *Kpn*I-*Hin*dIII (Sk 6652–7930); Ch-19: *Hin*dIII-*Xma*I (Sk 7930–9671); Ch-20: *Xma*I-*Asc*I* (Sk 9671–11,311); and Ch-21: *Stu*I-*Bam*HI (Sk 5771–7361). Chimeras Ch-4 (Sk 5045–11,311) and Ch-11 (Sk 6652–9671) were obtained by subcloning and ligation of chimeras Ch-10 and Ch-9 or Ch-18 and Ch-19, respectively (Fig. 1). All chimeric constructs were cloned into the HSV-1 amplicon vector pHSVprPUC (gift of Dr. Howard Federoff, University of Rochester, Rochester, NY) and packaged into HSV1 virions using a helper virus-free packaging system (Fraefel et al., 1996; Wang et al., 2000).

Cell culture and infection

1B5 cells (RyR1, RyR2, and RyR3 null) were cultured on Matrigel (BD Bioscience, San Jose, CA) coated 96-well plates (Costar, Corning, Acton, MA) in DMEM 20% FBS, 100 μg/ml streptomycin sulfate, 100 u/ml penicillin-G in 5% CO_2. After reaching 60–70% confluence cells were allowed to differentiate into myotubes for four to five days by changing the growth medium to DMEM containing 5% heat-inactivated horse serum-

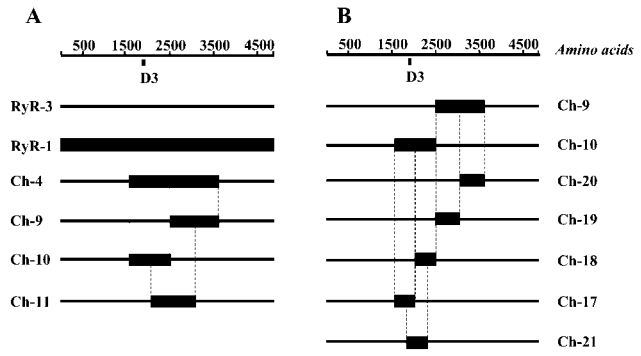

FIGURE 1 Schematic representation of the structure of chimeric RyR1/RyR3 receptor. The boxed areas indicate the regions of RyR3 replaced with the corresponding portion of RyR1. Numbers refer to the amino acids of RyR1 (R1) and RyR3 (R3) constituting each chimera. (*A*) Ch-4: R3(1-1577)-*R1(1681-3770)*-R3(3620-4873); Ch-9: R3(1-2507)-*R1(2642-3770)*-R3(3620-4873); Ch-10: R3(1-1577)-*R1(1681-2641)*-R3(2508-4873); Ch-11: R3(1-2083)-*R1(2218-3223)*-R3(3089-4873). (*B*) Ch-17: R3(1-1577)-*R1(1681-2217)*-R3(2083-4873); Ch-18: R3(1-2083)-*R1(2218-2643)*-R3(2508-4873); Ch-19: R3(1-2507)-*R1(2644-3223)*-R3(3089-4873); Ch-20: R3(1-3088)-*R1(3224-3770)*-R3(3620-4873); and Ch-21: R3(1-1797)-*R1(1924-2446)*-R3(2618-4873). D3 depicts position of high divergence sequence.

100 μg/ml streptomycin sulfate, 100 u/ml penicillin-G in 23% CO_2. Wells containing differentiated myotubes were infected with 3×10^4 virion particles containing RyR1/RyR3 chimeric cDNAs for 2 h, and then cultured for 24–48 h before imaging.

Calcium imaging

Differentiated 1B5 myotubes were loaded with 5 μM Fluo-4AM (Molecular Probes, Eugene, OR) at 37°C, for 20 min in imaging buffer (125 mM NaCl, 5 mM KCl, 2 mM $CaCl_2$, 1.2 mM $MgSO_4$, 6 mM glucose, and 25 mM HEPES, pH 7.4) supplemented with 0.05% BSA. Depolarization was performed by perfusion with five to seven volumes of K^+ buffer (50 mM NaCl, 80 mM KCl, 2 mM $CaCl_2$, 1.2 mM $MgSO_4$, 6 mM glucose, and 25 mM HEPES, pH 7.4) using a Multivalve Perfusion System (Automate Scientific, Oakland, CA). When appropriate, to make certain that the responses seen were the result of skeletal-type E-C coupling, the imaging and K^+ depolarization buffers were made nominally Ca^{2+} free (~5 μM free Ca^{2+}) and supplemented with 0.5 mM Cd^{2+} and 0.1 mM La^{3+} to prevent possible Ca^{2+} entry from the extracellular medium into the cells. Because of difficulties removing Cd^{2+} and La^{3+} from the wells, all the experiments were first carried out in Ca^{2+}-containing medium and then in Ca^{2+}-free medium plus Cd^{2+} and La^{3+}. Imaging was performed at 496 nm and data were collected at 30 fps with an intensified 12-bit digital intensified CCD (Stanford Photonics, Stanford, CA) and the data analyzed using QED Camera Plug-in package (QED Imaging, Pittsburgh, PA). A caffeine dose response curve was performed to evaluate the function of all of the chimeric constructs. Different caffeine concentrations were assayed in imaging buffer in the presence of extracellular Ca^{2+}. Because of the fact that low caffeine concentrations can induce brief Ca^{2+} transients having peak amplitudes near to those reached by higher caffeine concentration but a much smaller total Ca^{2+} release, we found that the average fluorescence of the calcium transient better represents the total Ca^{2+} transient behavior. To compare different experiments, individual average fluorescence was normalized to the maximal fluorescence obtained in the same cell (obtained by the addition of 5 mM or 20 mM caffeine for RyR3 and RyR1, respectively). To compare the efficiency of the different chimeras in restoring E-C coupling the normalized average fluorescence of the KCl-induced Ca^{2+} transient (Figs. 3 *C* and 4 *C*) was determined only in those cells in which E-C coupling was restored. Data are presented as mean ± SE calculated using Excel software (Microsoft Office 2001, Microsoft, Seattle WA). Differences among the data were evaluated for statistical significance using a one-way Kruchall-Wallace ANOVA (nonparametric) analysis (GraphPad Software, San Diego, CA).

Membrane preparation and immunoblotting

Crude membrane preparations were made 36 h after infection from 1B5 myotubes that had been allowed to differentiate for five days and were then transduced with different constructs. Myotubes were harvested in harvest buffer (137 mM NaCl, 3 mM KCl, 8 mM Na_2HPO_4, 1.5 mM KH_2PO_4, pH 7.2, and 0.6 mM EDTA) from 10–15 100-mm plates and centrifuged for 10 min at $250 \times g$. The pellet was resuspended in buffer consisting of 250 mM sucrose, 10 mM HEPES pH 7.4, supplemented with 1 mM EDTA, 10 μg/ml leupeptin, 0.7 μg/ml pepstatin A, 5 μg/ml aprotinin, and 0.1 mM PMSF and then homogenized using a Polytron cell disrupter (Brinkmann Instruments, Westbury, NY). The whole cell homogenates were centrifuged for 20 min at $1500 \times g$, and the supernatants were collected and recentrifuged for 60 min at $100{,}000 \times g$ at 4°C. The membranes were finally resuspended in 250 mM sucrose, 20 mM HEPES, pH 7.4, frozen in liquid N_2, and stored at −80°C. SDS-polyacrylamide gel electrophoresis (Laemmli 1970) was performed on proteins from the crude homogenates as described previously. Immunoblots were incubated with monoclonal antibody 34C (Airey and Sutko, ISHB, University of Iowa), which recognizes both RyR1 and RyR3, and then incubated with horseradish-peroxidase-conjugated goat anti-mouse secondary antibody. Immunoreactive proteins were developed with SuperSignal ultra chemoluminescent substrate (Pierce, Rockford, IL).

[^{3}H]-Ryanodine binding assay

High affinity binding of [^{3}H]-ryanodine (56 Ci/mmol; New England Nuclear, Boston, MA) to crude membrane extracts (0.05–0.15 mg/ml) was performed in the presence of 1M KCl, 20 mM HEPES pH 7.4, and 5 nM [^{3}H]-ryanodine in the presence of 100 μM free Ca^{2+}. The binding reaction was initiated by the addition of cell membranes to the medium and the mixture was permitted to equilibrate at 37°C for 3 h. Nonspecific binding was assessed in the presence of 5 μM unlabeled ryanodine. Separation of bound and free ligand was performed by rapid filtration through Whatman GF/B glass fiber filters using a Brandel cell harvester (Gaithersburg, MD). Filters were washed with three volumes of 0.5 ml ice-cold wash buffer containing 20 mM Tris-HCl, 1M KCl, and 100 μM $CaCl_2$, pH 7.1, and placed into vials with 5 ml scintillation cocktail (Ready Safe; Beckman Instruments, Fullerton, CA). The [^{3}H]-ryanodine remaining on the filters was quantified by liquid scintillation spectrometry.

RESULTS

Previous studies using chimeric RyR1/RyR2 receptors have identified two adjacent regions of RyR1, chimera R10 (RyR1 residues 1635–2636) and chimera R9 (RyR1 residues 2659–3720), involved in mediating the reciprocal interaction between RyR1 and DHPR (Nakai et al., 1998a). Whereas chimera R10 was able to both mediate skeletal-type E-C coupling and enhance Ca^{2+} channel activity, R9 was only able to enhance Ca^{2+} channel function. Based on this finding, and to identify the regions of RyR1 responsible for supporting skeletal-type E-C coupling, we designed different cDNAs constructs encoding chimeric receptors, in which selected regions of RyR1 were inserted in frame into the corresponding sequence of RyR3.

Accordingly, we designed two series of chimeric receptors. The first series, chimeras Ch-4, Ch-9, Ch-10, and Ch-11 (Fig. 1 *A*), includes receptors containing RyR1 regions formerly defined as essential for the interaction of RyR1/DHPR (namely R4, R9, and R10 in Nakai et al., 1998a). The second series, chimeras Ch-17, Ch-18, Ch-19, Ch-20, and Ch-21 (Fig. 1 *B*), was intended to further refine the regions of RyR1 directly involved in conferring on RyR1 the ability to support skeletal-type E-C coupling.

Transient expression of chimeric RyR cDNAs

In earlier studies we have shown that 1B5 dyspedic cells express all the key proteins needed for E-C coupling, but they lack expression of both RyR1 and RyR3 (Moore et al., 1998). Expression of the receptors in 1B5 myotubes was achieved using roughly equivalent levels of HSV-1 virion particles containing the chimeric cDNAs. Transient expression of the constructs was detected with monoclonal antibody 34C, which recognizes a conservative RyR epitope (Airey et al., 1990; Tong et al., 1997) that allows comparable identification of all three RyR isoforms (Airey et al., 1993b). Transduction of 1B5 dyspedic myotubes with virion particles containing *wt*RyR1, *wt*RyR3, or any of the chimeric constructs led to a high percentage of myotubes expressing

RyRs. Immunostaining using 34C antibody showed that 50–60% of the transduced myotubes displayed a punctate pattern of labeling (data not shown), previously shown as characteristic of RyRs properly localized at peripheral junctions (i.e., junctional SR/plasma membrane boundary, Protasi et al., 2000).

The Western blot in Fig. 2 *A* shows that membrane extracts from myotubes transduced with *wt*RyR1 or *wt*RyR3 expressed high molecular weight proteins, with RyR3 exhibiting a slightly higher mobility than RyR1 as has been previously shown for both *wt* and recombinant proteins (Chen et al., 1997; Fessenden et al., 2000; Murayama and Ogawa, 1997). Consistently, each of the RyR1/RyR3 chimeras expressed a high molecular weight protein with no evident differences in their molecular size as compared to their *wt*RyR3 parent, indicating that the insertion of different regions of RyR1 into the RyR3 sequence did not result in apparent change in size of the chimeric receptors. Variations in the level of expression of full-length RyR in any given culture were observed. Cultures expressing *wt*RyR1 consistently presented a lower level of expression than those expressing *wt*RyR3 or the chimeric constructs. This was further confirmed by [^{3}H]-ryanodine binding experiments (see below). Similar findings have been seen in heterologous cells expressing RyR2 and RyR3 (Du et al., 1998; Rossi et al., 2002). Despite this we did not see any significant differences in the morphology of the expression pattern of all constructs when we examined the cells using immunohistochemistry. In addition, slight differences in the level of the expression were also observed among the chimeric constructs (Fig. 2 *A*).

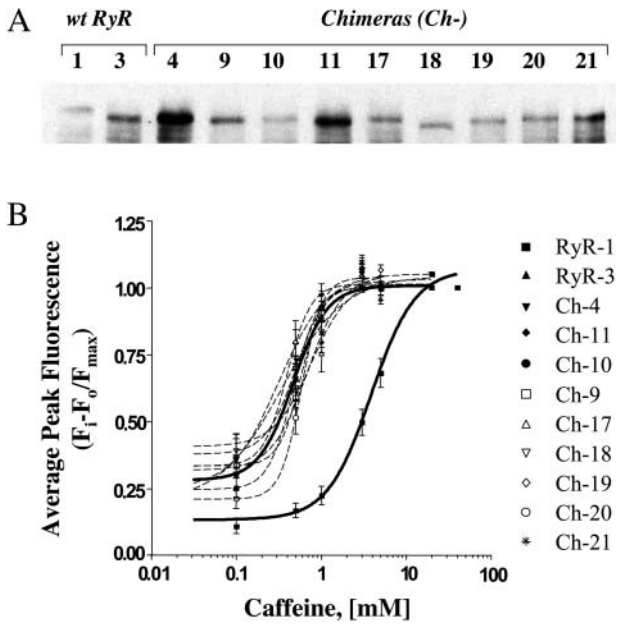

FIGURE 2 Structural/functional characterization of chimeric receptors. (*A*) Western blot analysis of the proteins expressed by transduced myotubes. 10 μg/lane of protein were used for each of the samples, with the exception of RyR1, which is 40 μg/lane. Numbers 1 and 3 represent *wt*RyR1 and *wt*RyR3 respectively, and 4–21 the remaining chimeric receptors. Expressed receptors were detected with mAb 34C. (*B*) Caffeine dose response of Fluo-4 loaded myotubes expressing *wt*- and chimeric receptors. Average fluorescence (see Materials and Methods) represents the mean fluorescence of 22–69 cells from three independent experiments. Results are presented as average ± SE. EC_{50} values were obtained by fitting the average data to a statistical dose response equation (Prism, Graphpad Software).

Caffeine dose response

Caffeine dose response curves were performed on Fluo 4-loaded cells to evaluate the functionality of the chimeric proteins expressed in the 1B5 myotubes. To make certain that any difference in the EC_{50} between constructs represents an actual difference in the properties of the channels and not the result of differential levels of expression, all EC_{50} values for caffeine were calculated from three independent experiments using three different cultures and at least two different viral stocks to transduce the cells. Average calcium transient fluorescence (see Materials and Methods) was normalized to the maximal response to caffeine (5 mM for RyR3 and 20 mM for RyR1).

In agreement with previous studies (Fessenden et al., 2000) we found that myotubes expressing *wt*RyR3 and *wt*RyR1 displayed different sensitivities to caffeine (Fig. 2 *B*), with RyR3 being more sensitive than RyR1. There was a significant difference in the caffeine EC_{50} between RyR1 and RyR3 (EC_{50} = 3.92 mM versus 0.47 mM, respectively, Table 1). Only small differences in the caffeine EC_{50} were observed among chimeric receptors and like *wt*RyR3 all chimeras had EC_{50} values below 1 mM. Statistical analysis showed no significant difference in caffeine EC_{50} ($p > 0.05$) between *wt*RyR3 and any of the chimeric constructs assayed. However, all the chimeric constructs had a significantly lower EC_{50} for caffeine than *wt*RyR1 ($p < 0.05$).

TABLE 1 Density of specific [^{3}H]-ryanodine-binding sites (pmol/mg) and cellular responses to caffeine (EC_{50}) for 1B5 myotubes expressing *wt*- and chimeric receptors

Construct	*pmol* [^{3}H]-ryanodine bound/mg protein ± SD	*n*	Caffeine EC_{50} mM
*wt*RyR1	0.154* ± 0.012	6	3.92*
*wt*RyR3	0.853* ± 0.130	6	0.47*
Ch-4	1.414 ± 0.313	6	0.34
Ch-9	0.849 ± 0.062	3	0.58
Ch-10	0.734 ± 0.063	3	0.47
Ch-11	1.841 ± 0.123	3	0.78†‡
Ch-17	0.565 ± 0.057	6	0.63‡
Ch-18	0.599 ± 0.517	3	0.51‡
Ch-19	1.523 ± 0.075	3	0.32
Ch-20	1.277 ± 0.056	3	0.58
Ch-21	1.823 ± 0.347	6	0.39†

SD, standard deviation; *n*, number of independent determinations.
*$p < 0.001$
†$p < 0.001$
‡$p > 0.05$

[^{3}H]-Ryanodine binding to chimeric constructs

To further evaluate the functionality and the level of expression of the chimeric constructs we performed [^{3}H]-ryanodine binding experiments. Specific [^{3}H]-ryanodine binding was assayed in vesicles from myotubes expressing *wt*-RyR1 and RyR3 and was compared to the binding to all chimeric receptors. Table 1 shows maximal [^{3}H]-ryanodine binding in the presence of 1M KCl and 100 μM free Ca^{2+}. Under these conditions *wt*RyR3 demonstrated specific binding to ryanodine, ~5.5-fold higher than *wt*RyR1, a finding consistent with the Western blot analysis showing that RyR3-transduced myotubes always expressed a higher level of receptor/mg total protein than RyR1-transduced myotubes. This result is consistent with previous reports where similar differences in [^{3}H]-ryanodine binding have also been reported for recombinant RyR1 and RyR3 expressed in HEK cells (Rossi et al., 2002). Unlike RyR1/RyR2 chimeras, all RyR1/RyR3 chimeric receptors showed high affinity [^{3}H]-ryanodine binding, with a B_{max} similar to *wt*RyR3 and 5- to 12-fold higher than *wt*RyR1 indicating a direct correlation between the amount of receptor expressed and [^{3}H]-ryanodine B_{max}, observed.

Correlation of [^{3}H]-ryanodine B_{max} and caffeine EC_{50}

There was no relationship between [^{3}H]-ryanodine B_{max} and caffeine EC_{50}. Table 1 shows that constructs with equivalent levels of [^{3}H]-ryanodine B_{max} can display significant differences in caffeine EC_{50} (i.e., chimeras Ch-21 and Ch-11) conversely; constructs with up to threefold difference in their average [^{3}H]-ryanodine B_{max} had the same caffeine EC_{50} (i.e., chimeras Ch-11, Ch-17, and Ch-18). Based on these results it seems unlikely that the higher levels of expression observed with RyR3 and all chimeras can account for the increased caffeine sensitivity observed in these constructs and that this decrease in EC_{50} is due to an intrinsic structural difference somewhere in their common RyR3 backbone.

Restoration of E-C coupling by chimeric receptors

Myotubes expressing *wt*RyR1 or *wt*RyR3 loaded with Fluo-4AM were tested for their response to 80 mM KCl and 20 or 5 mM caffeine (Fig. 3) respectively. Upon application of KCl for 5–10 s, robust intracellular Ca^{2+} transients were observed in 52/52 myotubes expressing RyR1 ($n = 3$, independent experiments), both in the presence and the absence of extracellular Ca^{2+}. Unlike myotubes expressing *wt*RyR1, in the presence of 2 mM Ca^{2+}, myotubes expressing *wt*RyR3 responded to KCl depolarization either with a very weak and slow increase in $[Ca^{2+}]_i$ or had no detectable transient (Fig. 3 *A*). Only a few myotubes (16/40 myotubes, [$n = 3$] Fig. 3 *B*) expressing RyR3 had a Ca^{2+} transient with an amplitude higher than 10% of the maximal Ca^{2+} release induced by 5 mM caffeine, and none showed a transient which resembled the transients seen with RyR1 (Fig. 3, *B* and *C*).

Although all myotubes expressing RyR3 were able to respond to 5 mM caffeine in the presence of Cd^{2+} and La^{3+}, no depolarization-induced Ca^{2+} transients were observed under these conditions (0/40 myotubes assayed [$n = 3$], Fig. 3). This suggests that the small depolarization-induced increase of $[Ca^{2+}]_i$ observed in the presence of 2 mM extracellular Ca^{2+} most likely represents sarcolemmal Ca^{2+} influx rather than Ca^{2+} release from the SR. These results also confirm the fact that, unlike RyR1, RyR3 is not able to

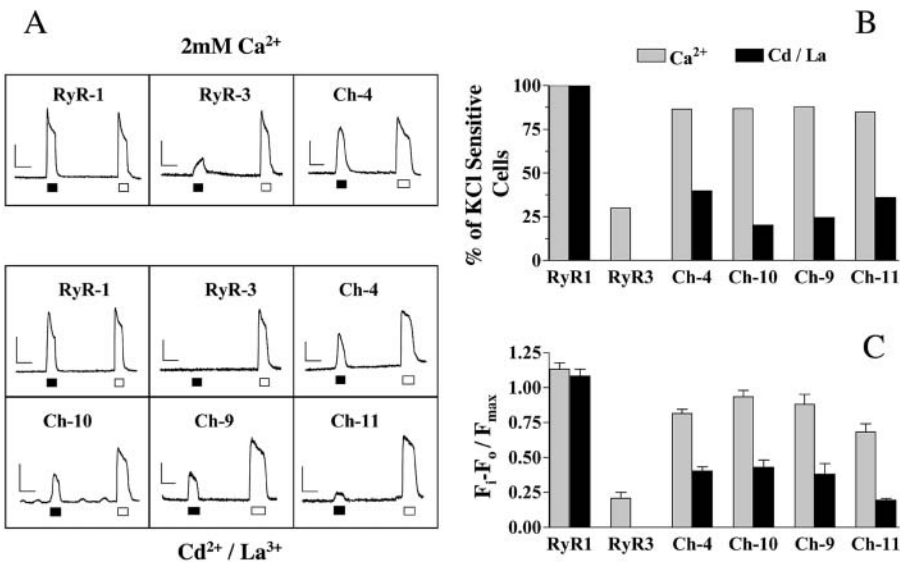

FIGURE 3 Chimeric receptors Ch-4, Ch-9, Ch-10, and Ch-11 support E-C coupling in dyspedic myotubes. (*A*) Representative Ca^{2+} transients in response to KCl and caffeine of 1B5 myotubes expressing *wt*- or chimeric receptors. Cells were exposed to depolarization with 80 mM KCl (*black box*) or 5–20 mM caffeine (*white box*) for 5–10 s in the absence and in the presence of 0.5 mM Cd^{2+} and 0.1 mM La^{3+}. (*B*) Percentage of cells transduced with *wt*- or chimeric receptors that respond to depolarization. The number of cells was determined either in the presence (*gray bars*) or in the absence (*black bars*) of 2 mM Ca^{2+} plus Cd^{2+} and La^{3+} in the extracellular medium. (*C*) Normalized peak fluorescence of KCl-induced Ca^{2+} transients of *wt*- and chimeric constructs, in the presence and in the absence of $[Ca^{2+}]_o$. These data represent the average fluorescence of only those cells that showed a response to KCl in *C*. The horizontal bar represents 10 s; the vertical bar represents 250 au of Fluo-4 fluorescence.

restore skeletal-type E-C coupling to dyspedic myotubes (Airey et al., 1993a; Fessenden et al., 2000).

Fig. 3 *A* shows that the expression of chimera Ch-4 in dyspedic myotubes led to the restoration of depolarization-induced Ca^{2+} transients, both in the presence (64/74 myotubes, $n = 4$) and absence (45/113 myotubes, $n = 5$) of extracellular Ca^{2+}. This finding is consistent with previous studies reporting that the sequence between amino acid 1681–3770 of RyR1 contains the essential region required to confer skeletal-type E-C coupling on RyR2 (Nakai et al., 1998a). Interestingly both the number of cells responding (Fig. 3 *B*) and the magnitude of the Ca^{2+} transients (Fig. 3, *A* and *C*) restored by Ch-4 in the absence of extracellular Ca^{2+} were always smaller than those observed in the presence of 2 mM Ca^{2+}.

Like Ch-4, expression of chimeras containing smaller segments of RyR1 such as Ch-10 (amino acid 1681–2641) and Ch-9 (amino acid 2642–3770) were equally able to the restore skeletal-type E-C coupling in dyspedic myotubes. In the presence of Cd^{2+} and La^{3+} both of these chimeras had a similar frequency of E-C coupling restoration (24/119 myotubes [$n = 7$] and 14/57 myotubes [$n = 6$], for Ch-10 and Ch-9 respectively) and both Ch-9 and Ch-10 had Ca^{2+} transients of similar magnitude to each other and to Ch-4 (Fig. 3 *C*). Ch-11, which encompasses residues 2218–3223 of RyR1, was also able to restore E-C coupling in both the presence (79/93 myotubes, $n = 5$) and absence (48/133 myotubes, $n = 6$) of extracellular Ca^{2+}. However the kinetics of the Ca^{2+} transient induced by depolarization in the presence of Cd^{2+} and La^{3+} were always slower in Ch-11-expressing cells than the kinetics of release in cells expressing Ch-4, Ch-10, or Ch-9 (Fig. 3 *A*). Additionally, Ca^{2+} transients observed in Ch-11-expressing cells were consistently smaller than those of the other chimeras indicating a reduced ability to restore skeletal E-C coupling (Fig. 3 *C*). Altogether, these data indicate that two adjacent regions of RyR1 can independently engage skeletal-type E-C coupling observed in chimera Ch-4.

To better define the essential sequences of RyR1 required to confer skeletal-type E-C coupling to RyR1/RyR3 chimeras, we further divided chimera Ch-10 into two smaller constructs, Ch-17 (RyR1: 1681–2217) and Ch-18 (RyR1: 2218–2643), and Ch-9 into chimeras Ch-19 (RyR1; 2644–3223) and Ch-20 (RyR1; 3224–3770). Fig. 4, *B* and *C* show that both chimera Ch-17 and Ch-18 were capable of restoring E-C coupling in the presence of 2 mM extracellular Ca^{2+}, where strong Ca^{2+} transients were observed in 44/51 myotubes ($n = 3$) expressing Ch-17 and 29/37 myotubes ($n = 3$) expressing Ch-18. However, the same cells failed to display any E-C coupling in the absence of extracellular Ca^{2+} and presence of Cd^{2+} and La^{3+} (Fig. 4, *A–C*). Unlike cells expressing Ch-17 and Ch-18, myotubes expressing chimera Ch-19 retained their ability to restore E-C coupling regardless of the presence of extracellular Ca^{2+}, where 15/71 myotubes assayed ($n = 3$) were able to restore skeletal-type

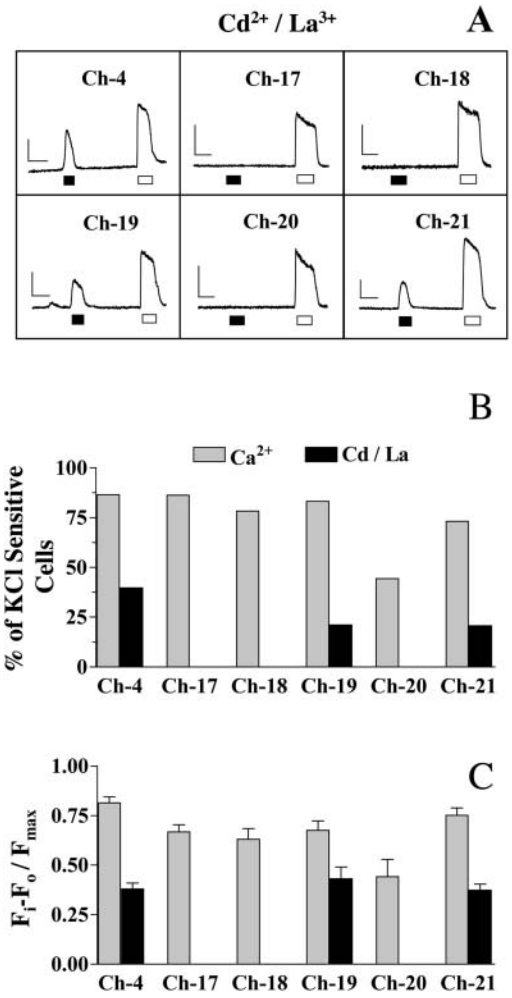

FIGURE 4 Chimeras Ch-19 and Ch-21 support skeletal-type E-C coupling in dyspedic myotubes. (*A*) Representative calcium transients induced by depolarization with 80 mM KCl (*black box*) and 5 mM caffeine (*white box*) of dyspedic myotubes expressing chimeric receptors Ch-17, Ch-18, Ch-19, Ch-20, and Ch-21. Fluorescent records represent only those responses measured in the absence of extracellular Ca^{2+} with added Cd^{2+} and La^{3+}. (*B*) The percentage of cells transduced with chimeric receptors that respond to depolarization. The number of cells was determined either in the presence (*gray bars*) or in the absence (*black bars*) of 2 mM Ca^{2+} plus Cd^{2+} and La^{3+} in the extracellular medium. (*C*) Normalized peak fluorescence of KCl-induced Ca^{2+} transients of chimeras Ch-4, Ch-17, Ch-18, Ch-19, Ch-20, and Ch-21, in the presence and in the absence of $[Ca^{2+}]_o$. These data represent the average fluorescence of only those cells that showed a response to KCl in *C*. The horizontal bar represents 10 s; the vertical bar represents 250 au of fluorescence.

E-C coupling in the presence of Cd^{2+} and La^{3+}, the same percentage of restoration that was accomplished by chimera Ch-9. Chimera Ch-20 displayed only a weak restoration of E-C coupling, even in the presence of extracellular Ca^{2+} (Fig. 4, *B* and *C*), suggesting that chimera Ch-19 holds the entire sequence responsible for the interaction with the DHPR previously identified in Ch-9.

To evaluate whether a region containing parts of both chimeras Ch-17 and Ch-18 was responsible for the activity

displayed by chimera Ch-10, we designed chimera Ch-21- encompassing residues 1924–2446 of RyR1. Fig. 4, *B* and *C* show that 31/149 myotubes ($n = 5$) expressing Ch-21 were able to engage skeletal-type E-C coupling that was missed by chimeras Ch-17 and Ch-18.

DISCUSSION

In previous reports, using chimeric RyR1/RyR2 ryanodine receptors (Nakai et al., 1998a; Protasi et al., 2002) two regions of RyR1 were identified that can independently mediate the reciprocal interaction with skeletal DHPR. One of these was more efficient in restoring skeletal-type E-C coupling and the other was more efficient in stimulating the α_{1S}-DHPR to assemble in tetrads. Both were equally able to enhance DHPR Ca^{2+} current compared to dyspedic cells or cells expressing RyR2. To validate these results in this work we have expressed the same regions of RyR1 in a RyR3 background using a similar experimental approach. Expressing chimeric RyR1/RyR3 ryanodine receptors in dyspedic 1B5 myotubes we have demonstrated that the regions of RyR1 previously shown to restore skeletal-type E-C coupling to RyR2 were also able to confer similar properties to RyR3. This result supports the hypothesis that this central domain contains at least part if not all of the critical regions of RyR1 needed to provide skeletal-type E-C coupling, regardless of the background in which it is expressed.

Converging on smaller domains within chimeras Ch-10 and Ch-9 we showed that chimera Ch-21 (amino acids 1924–2446) and chimera Ch-19 (amino acids 2644–3223) are the critical regions necessary to contribute all of the skeletal E-C coupling function. Interestingly, these two domains neither overlap nor are adjacent in the primary sequence, but are separated from each other by 427 amino acids. Whether these domains represent two independent topographic regions of RyR1 that independently interact with the α_{1S}-DHPR, or they are configured into a single contiguous domain during protein folding, still remains to be resolved.

We found by Western blot analysis that, compared to RyR1, there was an almost consistently increased level of receptor expression in the RyR3-based constructs and that this correlated with [^{3}H]-ryanodine B_{max} in all constructs. Some of the cause for the difference in binding levels between RyR1 and RyR3 constructs and differences in binding among RyR3 chimeras is that different viral stocks used to transduce the cells had different viral titers. This can potentially lead to large differences in the number of cells expressing any RyR in any culture and is the reason that [^{3}H]-ryanodine B_{max} levels were not consistent among membrane preparations from different cultures expressing the same construct. The remainder of the difference in expression levels can be attributed to the fact that levels of RyR1 expression has been consistently been shown to be lower than RyR2 and RyR3 when these constructs are expressed in heterologous expression systems (Du et al., 1998; Rossi et al., 2002). At first glance it appears that this difference in expression might be the cause of the increased sensitivity to caffeine seen in cells expressing RyR3-based constructs. This proved not to be the case. Using two separate Ch-18 viral stocks, EC_{50} for caffeine was the same in both; in their respective membrane preps, the first prep showed receptor expression levels and [^{3}H]-ryanodine B_{max} similar to those of RyR1, whereas in the second receptor, expression levels and [^{3}H]-ryanodine B_{max} were 10-fold higher than RyR1. Our results are consistent with previous findings that recombinant *wt*RyR1 and *wt*RyR3 expressed in myotubes (Fessenden et al., 2000) and HEK293 cells (Rossi et al., 2002) displayed similar differential caffeine sensitivities. Although it is still unknown what domain of the receptor accounts for this difference, the fact that all of the constructs expressing the highest caffeine sensitivity shared common N-terminal and C-terminal regions make apparent that the increased caffeine sensitivity must be determined by one of these domains.

An intriguing result was the fact that in the presence of 2 mM Ca^{2+} all chimeric receptors except Ch-20 presented a near normal restoration of depolarization-induced E-C coupling. Furthermore, unlike *wt*RyR1 the depolarization-induced Ca^{2+} transients in the presence of extracellular Ca^{2+} were always stronger for all of the chimeras than in the absence of the cation, indicating that Ca^{2+} influx through the DHPR can make an important contribution to depolarization-induced Ca^{2+} release signals. By comparison, RyR3-expressing myotubes presented only a minimal level of coupling and the amplitudes of the depolarization-induced Ca^{2+} transients, when present at all, were significantly smaller and displayed different kinetics than the depolarization-induced transients observed in cells expressing RyR1 or any of the chimeric constructs except Ch-20. The most likely explanation for the differences in the amplitude of the depolarization-induced Ca^{2+} transients in the presence of extracellular Ca^{2+} is that the RyR3 chimeras other than Ch-20, unlike *wt*RyR3, are able to restore bidirectional signaling with the DHPR and thus increase its current density similar to the increase seen with RyR1/RyR2 chimeras (Nakai et al., 1998a).

The finding that chimera Ch-17 (amino acids 1681–2217), which contains the highly divergent D3 domain, was not able to restore skeletal-type E-C coupling suggests that this domain of RyR1 (amino acids 1872–1923) does not play an essential role in E-C coupling. This is consistent with the report of Proenza et al. (2002) who found that chimera *R16 reverse*, in which D3 domain of RyR1 was replaced with the corresponding region of RyR2, retained a normal ability to mediate bidirectional signaling during E-C coupling. Furthermore, chimera *R16* (RyR1 amino acids 1837–2154) was only partially able to restore skeletal-type E-C coupling when expressed in a RyR2 background (Proenza et al., 2002). Despite the similarities in the function of RyR2 and RyR3 chimeras there are significant differences that must be

explained. The most significant difference we found was that under identical experimental conditions as those described in this study the RyR1/RyR2 chimeras containing RyR1 sequences within amino acids 1635–3720 (i.e., chimeras R4, R10, and R9; Protasi et al., 2002) consistently showed a more robust skeletal-type E-C coupling signal than their homologous chimeras (Ch-4, Ch-10, and Ch-9 respectively) in a RyR3 background. It is possible that this decreased efficiency of depolarization-induced response can be attributed simply to possible protein misfolding of any given chimera. But, because there was basically no difference in caffeine sensitivity, [^{3}H]-ryanodine B_{max}, or molecular size of any of the chimeric RyR3 receptors compared with *wt*RyR3, this strongly suggests that the substitution of RyR1 sequence in the different regions of these chimeric receptors did not alter their overall protein conformation. Therefore the differences observed between chimeras with RyR2 and RyR3 backgrounds must come from the fact that the amino acid sequences of RyR2 and RyR3 are not equivalent.

Although the overall amino acid sequence identity among the RyRs subtypes is 67–70%, there are several regions where the amino acid sequences significantly diverge (domains D1, D2, and D3). A close analysis of the sequence in the proposed foot region reveals the existence of several other short regions in which RyR1 shows a high homology with RyR2 but very low homology with RyR3. It is likely that some, or all, of these regions shared by RyR1 and RyR2 but not RyR3, represent domains that could either be critical for E-C coupling or are needed to properly expose the critical E-C coupling domains to the DHPR. In this regard, particularly interesting is the highly divergent domain, D2 (RyR1 residues 1342–1403 and RyR2 1316–1400). This region presents a very low homology between RyR1 and RyR2 but the corresponding sequence in RyR3 is almost completely absent. Yamazawa et al. (1997) have shown that deletion of this region from RyR1 completely ablated electrically-evoked Ca^{2+} release in cultured myotubes without affecting caffeine-induced Ca^{2+} release, suggesting that either this region plays a critical role in E-C coupling or that the deletion of D2 region disrupts the structure of RyR1 sufficiently to prevent antegrade DHPR/RyR1 interaction. Yamazawa also found that substitution of the D2 region of RyR1 with the corresponding region of RyR2 could support electrically evoked Ca^{2+} release, suggesting an equivalence of this domain between the type-1 and type-2 receptors. The absence of this domain in our RyR1/RyR3 constructs may very well at least partially explain the differences observed between chimeras with RyR2 and RyR3 backgrounds, and in some regards makes it surprising that any of the RyR3-based chimeras showed any depolarization-induced Ca^{2+} release at all. A study of the role of D2 domain in the E-C coupling restoration by chimeric RyR1/RyR3 receptors is currently on going.

Previous attempts to find region(s) of RyR1 involved in interaction with the α_{1S}-DHPR have led to the identification of RyR1 domains, which are both in the same or at different locations in the primary sequence than those proposed by Nakai et al. (1998a) or used in this study. Using a yeast two-hybrid system, Proenza et al. (2002) reported that region sR16 of RyR1 (residues 1837–2168) was able to interact with DHPR α_{1S} II–III loop (residues 720–765) but either failed to restore or restored only weak skeletal-type E-C coupling when it was expressed in an RyR2 background. Using a protein affinity chromatography approach, Leong and MacLennan (1998a) have reported that a peptide fragment containing amino acids 922–1112 of RyR1 was able to bind skeletal but not cardiac II–III loop fused to GST. Furthermore, the same domain also showed the ability to bind III–IV loop from skeletal muscle (Leong and MacLennan, 1998b,c). Although it has been shown that only 46 amino acids in the α_{1S}-DHPR II–III loop are required to support skeletal E-C coupling (Grabner et al., 1999) other in vitro studies have suggested that in addition to the II–III loop, other regions of the α_{1S}-DHPR and other DHPR subunits may engage in physical contact with RyR1 (Beurg et al., 1997; Leong and MacLennan, 1998c; Mouton et al., 2001; Strube et al., 1996). Taken altogether, the accumulated information supports the idea that several non-contiguous domains of RyR1 are required to support normal bidirectional interaction between RyR1 and DHPR during the E-C coupling. The fact that these domains are broadly spread into the primary sequence of RyR1 makes it somewhat unlikely that all of them come together to configure a single interaction domain. However, until the three-dimensional structure of both RyR1 and the entire triad complex is determined at near-atomic resolution, it will be impossible to determine the actual location of these domains.

We thank Dr. S.R.W. Chen for kindly providing us with the HSV-RyR3 cDNA vector, and Dr. Y. Wang and Ms. R. Hirsh for their technical expertise and help in virus packaging.

This work was supported by National Institutes of Health grant PO1AR47605 to P.D.A. and I.N.P., and Fogarty International Center Fellowship F05TW05455 to C.F.P.

REFERENCES

Airey, J. A., M. D. Baring, C. F. Beck, Y. Chelliah, T. J. Deerinck, M. H. Ellisman, L. J. Houenou, D. D. McKemy, J. L. Sutko, and J. Talvenheimo. 1993a. Failure to make normal alpha ryanodine receptor is an early event associated with the crooked neck dwarf (cn) mutation in chickens. *Dev. Dyn.* 197:169–188.

Airey, J. A., C. F. Beck, K. Murakami, S. J. Tanksley, T. J. Deerinck, M. H. Ellisman, and J. L. Sutko. 1990. Identification and localization of two triad junctional foot protein isoforms in mature avian fast twitch skeletal muscle. *J. Biol. Chem.* 265:14187–14194.

Airey, J. A., M. M. Grinsell, L. R. Jones, J. L. Sutko, and D. Witcher. 1993b. Three ryanodine receptor isoforms exist in avian striated muscles. *Biochemistry*. 32:5739–5745.

Berchtold, M. W., H. Brinkmeier, and M. Muntener. 2000. Calcium ion in skeletal muscle: its crucial role for muscle function, plasticity, and disease. *Physiol. Rev.* 80:1215–1265.

Beurg, M., M. Sukhareva, C. Strube, P. A. Powers, R. G. Gregg, and R. Coronado. 1997. Recovery of Ca^{2+} current, charge movements, and

Ca^{2+} transients in myotubes deficient in dihydropyridine receptor beta 1 subunit transfected with beta 1 cDNA. *Biophys. J.* 73:807–818.

Chen, S. R., X. Li, K. Ebisawa, and L. Zhang. 1997. Functional characterization of the recombinant type 3 Ca^{2+} release channel (ryanodine receptor) expressed in HEK293 cells. *J. Biol. Chem.* 272:24234–24246.

Du, G. G., J. P. Imredy, and D. H. MacLennan. 1998. Characterization of recombinant rabbit cardiac and skeletal muscle Ca^{2+} release channels (ryanodine receptors) with a novel [^{3}H]ryanodine binding assay. *J. Biol. Chem.* 273:33259–33266.

Fessenden, J. D., Y. Wang, R. A. Moore, S. R. Chen, P. D. Allen, and I. N. Pessah. 2000. Divergent functional properties of ryanodine receptor types 1 and 3 expressed in a myogenic cell line. *Biophys. J.* 79:2509–2525.

Fraefel, C., S. Song, F. Lim, P. Lang, L. Yu, Y. Wang, P. Wild, and A. I. Geller. 1996. Helper virus-free transfer of herpes simplex virus type 1 plasmid vectors into neural cells. *J. Virol.* 70:7190–7197.

Grabner, M., R. T. Dirksen, N. Suda, and K. G. Beam. 1999. The II–III loop of the skeletal muscle dihydropyridine receptor is responsible for the bi-directional coupling with the ryanodine receptor. *J. Biol. Chem.* 274:21913–21919.

Ivanenko, A., D. D. McKemy, J. L. Kenyon, J. A. Airey, and J. L. Sutko. 1995. Embryonic chicken skeletal muscle cells fail to develop normal excitation-contraction coupling in the absence of the alpha ryanodine receptor. Implications for a two-ryanodine receptor system. *J. Biol. Chem.* 270:4220–4223.

Katoh, H., K. Schlotthauer, and D. M. Bers. 2000. Transmission of information from cardiac dihydropyridine receptor to ryanodine receptor: evidence from BayK 8644 effects on resting Ca^{2+} sparks. *Circ. Res.* 87:106–111.

Laemmli, U. K. 1970. Cleavage of structural proteins during the assembly of the head of bacteriophage T4. *Nature.* 227:680–685.

Leong, P., and D. H. MacLennan. 1998a. A 37-amino acid sequence in the skeletal muscle ryanodine receptor interacts with the cytoplasmic loop between domains II and III in the skeletal muscle dihydropyridine receptor. *J. Biol. Chem.* 273:7791–7794.

Leong, P., and D. H. MacLennan. 1998b. Complex interactions between skeletal muscle ryanodine receptor and dihydropyridine receptor proteins. *Biochem. Cell Biol.* 76:681–694.

Leong, P., and D. H. MacLennan. 1998c. The cytoplasmic loops between domains II and III and domains III and IV in the skeletal muscle dihydropyridine receptor bind to a contiguous site in the skeletal muscle ryanodine receptor. *J. Biol. Chem.* 273:29958–29964.

Moore, R. A., H. Nguyen, J. Galceran, I. N. Pessah, and P. D. Allen. 1998. A transgenic myogenic cell line lacking ryanodine receptor protein for homologous expression studies: reconstitution of Ry1R protein and function. *J. Cell Biol.* 140:843–851.

Mouton, J., M. Ronjat, I. Jona, M. Villaz, A. Feltz, and Y. Maulet. 2001. Skeletal and cardiac ryanodine receptors bind to the Ca^{2+}-sensor region of dihydropyridine receptor alpha(1C) subunit. *FEBS Lett.* 505: 441–444.

Murayama, T., and Y. Ogawa. 1997. Characterization of type 3 ryanodine receptor (RyR3) of sarcoplasmic reticulum from rabbit skeletal muscles. *J. Biol. Chem.* 272:24030–24037.

Nakai, J., R. T. Dirksen, H. T. Nguyen, I. N. Pessah, K. G. Beam, and P. D. Allen. 1996. Enhanced dihydropyridine receptor channel activity in the presence of ryanodine receptor. *Nature.* 380:72–75.

Nakai, J., T. Ogura, F. Protasi, C. Franzini-Armstrong, P. D. Allen, and K. G. Beam. 1997. Functional nonequality of the cardiac and skeletal ryanodine receptors. *Proc. Natl. Acad. Sci. USA.* 94:1019–1022.

Nakai, J., N. Sekiguchi, T. A. Rando, P. D. Allen, and K. G. Beam. 1998a. Two regions of the ryanodine receptor involved in coupling with L-type Ca^{2+} channels. *J. Biol. Chem.* 273:13403–13406.

Nakai, J., T. Tanabe, T. Konno, B. Adams, and K. G. Beam. 1998b. Localization in the II–III loop of the dihydropyridine receptor of a sequence critical for excitation-contraction coupling. *J. Biol. Chem.* 273:24983–24986.

Ottini, L., G. Marziali, A. Conti, A. Charlesworth, and V. Sorrentino. 1996. Alpha and beta isoforms of ryanodine receptor from chicken skeletal muscle are the homologues of mammalian RyR1 and RyR3. *Biochem. J.* 315:207–216.

Oyamada, H., T. Murayama, T. Takagi, M. Iino, N. Iwabe, T. Miyata, Y. Ogawa, and M. Endo. 1994. Primary structure and distribution of ryanodine-binding protein isoforms of the bullfrog skeletal muscle. *J. Biol. Chem.* 269:17206–17214.

Proenza, C., J. O'Brien, J. Nakai, S. Mukherjee, P. D. Allen, and K. G. Beam. 2002. Identification of a region of RyR1 that participates in allosteric coupling with the alpha(1S) (Ca(V)1.1) II–III loop. *J. Biol. Chem.* 277:6530–6535.

Protasi, F., C. Paolini, J. Nakai, K. Beam, C. Franzini-Armstrong, and P. Allen. 2002. Two separate regions of RyR-1 participate in the functional and structural interactions with DHPR's that allow skeletal type EC coupling. *Biophys. J.* 83:3230–3244.

Protasi, F., H. Takekura, Y. Wang, S. R. Chen, G. Meissner, P. D. Allen, and C. Franzini-Armstrong. 2000. RYR1 and RYR3 have different roles in the assembly of calcium release units of skeletal muscle. *Biophys. J.* 79:2494–2508.

Rios, E., M. Karhanek, J. Ma, and A. Gonzalez. 1993. An allosteric model of the molecular interactions of excitation-contraction coupling in skeletal muscle. *J. Gen. Physiol.* 102:449–481.

Rios, E., and G. Pizarro. 1991. Voltage sensor of excitation-contraction coupling in skeletal muscle. *Physiol. Rev.* 71:849–908.

Rossi, D., I. Simeoni, M. Micheli, M. Bootman, P. Lipp, P. D. Allen, and V. Sorrentino. 2002. RyR1 and RyR3 isoforms provide distinct intracellular Ca^{2+} signals in HEK 293 cells. *J. Cell Sci.* 115:2497–2504.

Schneider, M. F. 1994. Control of calcium release in functioning skeletal muscle fibers. *Annu. Rev. Physiol.* 56:463–484.

Slavik, K. J., J. P. Wang, B. Aghdasi, J. Z. Zhang, F. Mandel, N. Malouf, and S. L. Hamilton. 1997. A carboxy-terminal peptide of the alpha 1-subunit of the dihydropyridine receptor inhibits Ca^{2+}-release channels. *Am. J. Physiol.* 272:C1475–C1481.

Stange, M., A. Tripathy, and G. Meissner. 2001. Two domains in dihydropyridine receptor activate the skeletal muscle Ca^{2+} release channel. *Biophys. J.* 81:1419–1429.

Strube, C., M. Beurg, P. A. Powers, R. G. Gregg, and R. Coronado. 1996. Reduced Ca^{2+} current, charge movement, and absence of Ca^{2+} transients in skeletal muscle deficient in dihydropyridine receptor beta 1 subunit. *Biophys. J.* 71:2531–2543.

Tanabe, T., K. G. Beam, B. A. Adams, T. Niidome, and S. Numa. 1990. Regions of the skeletal muscle dihydropyridine receptor critical for excitation-contraction coupling. *Nature.* 346:567–569.

Tong, J., H. Oyamada, N. Demaurex, S. Grinstein, T. V. McCarthy, and D. H. MacLennan. 1997. Caffeine and halothane sensitivity of intracellular Ca^{2+} release is altered by 15 calcium release channel (ryanodine receptor) mutations associated with malignant hyperthermia and/or central core disease. *J. Biol. Chem.* 272:26332–26339.

Wang, Y., C. Fraefel, F. Protasi, R. A. Moore, J. D. Fessenden, I. N. Pessah, A. DiFrancesco, X. Breakefield, and P. D. Allen. 2000. HSV-1 amplicon vectors are a highly efficient gene delivery system for skeletal muscle myoblasts and myotubes. *Am. J. Physiol. Cell Physiol.* 278:C619–C626.

Wilkens, C. M., N. Kasielke, B. E. Flucher, K. G. Beam, and M. Grabner. 2001. Excitation-contraction coupling is unaffected by drastic alteration of the sequence surrounding residues L720–L764 of the alpha 1S II–III loop. *Proc. Natl. Acad. Sci. USA.* 98:5892–5897.

Yamazawa, T., H. Takeshima, M. Shimuta, and M. Iino. 1997. A region of the ryanodine receptor critical for excitation-contraction coupling in skeletal muscle. *J. Biol.Chem.* 272:8161–8164.